Zn–Cu-codoped SnO_2 nanoparticles: Structural, optical, and ferromagnetic behaviors*

Syed Zulfiqar[1,2], Zainab Iqbal[3], and Jianguo Lü(吕建国)[1,†]

[1] State Key Laboratory of Silicon Materials, School of Materials Science and Engineering, Zhejiang University, Hangzhou 310027, China
[2] Department of Physics, Abdul Wali Khan University, Mardan 23200, Khyber Pukhtunkhwa, Pakistan
[3] Institute of Chemical Sciences, University of Peshawar, Khyber Pukhtunkhwa, 25120, Pakistan

(Received 12 July 2017; revised manuscript received 9 September 2017; published online 20 November 2017)

Zn–Cu-codoped SnO_2 nanoparticles have been synthesized by chemical precipitation method. All nanoparticles are crystalline, with the average size increases from 2.55 nm to 4.13 nm as the calcination temperature increases from 400 °C to 600 °C. The high calcination temperature can enhance the crystalline quality and grain growth. The oxygen content decreases with decreasing calcination temperature; at a low temperature of 400 °C, Zn–Cu-codoped SnO_2 nanoparticles are in a rather oxygen-poor state having many oxygen vacancies. The optical band gap energies of Zn–Cu-codoped SnO_2 nanoparticles calcined at 400 °C and 600 °C are decreased from 3.93 eV to 3.62 eV due to quantum confinement effects. Both samples exhibit room-temperature ferromagnetism, with a larger saturation magnetization at 400 °C due to the presence of large density of defects such as oxygen vacancies. Zn–Cu-codoped SnO_2 nanoparticles exhibit large optical band gap energies and room temperature ferromagnetism, which make them potential candidates for applications in optoelectronics and spintronics.

Keywords: SnO_2 nanoparticles, Zn–Cu codoping, optical band gap energy, ferromagnetism

PACS: 61.46.Df **DOI:** 10.1088/1674-1056/26/12/126104

1. Introduction

The subject of great interest in case of nanoparticles is quantum size effect. In case of semiconductor nanoparticles, the band gap plays a vital role and the band gap structure is strongly dependent on size of nanoparticles.[1] According to the quantum confinement effect, the band gap increases as the size of nanoparticles reduces in the regime of nanometer. Therefore, it is very important to synthesize nanoparticles with desired sizes and properties. The common routes used for the synthesis of nanoparticles include sol–gel method,[2] hydrothermal technique,[3] polyol method,[4] chemical vapor deposition,[5] spray pyrolysis,[6] pulsed laser deposition,[7] high vacuum evaporation,[8] and co-precipitation.[9,10] The structural, optical, and magnetic properties of semiconductor nanoparticles are the main focus of researchers in recent years.[11,12] Semiconductor nanoparticles are the most suitable candidates with a range of variations in optical and magnetic properties having potential applications in photo catalysis, optoelectronics and spintronics.[13,14]

SnO_2 is one of the prominent metal oxide semiconductors with a direct band gap having band gap energy of 3.6 eV at room temperature. Its n-type conductivity is because of presence of oxygen vacancies in the rutile structure. The properties which make it very much valuable according to technological point of view are its high conductivity, transparency in visible light, high infrared reflectance, abundance in nature, and absence of toxicity. The properties of SnO_2 nanoparticles can be tuned largely by introducing impurity or dopant and forming defects in the matrix. Previously, the researchers have investigated the visible light response of SnO_2 by introduction of defects (tin interstitials, oxygen vacancies, crystal disorder and doping).[15,16] Due to its large surface-to-volume ratio and quantum confinement effects, nanocrystalline SnO_2 exhibits remarkable properties and has outstanding advantages of various operating temperatures and wide applications.

In this work, we have synthesized Zn–Cu-codoped SnO_2 nanoparticles by a co-precipitation method. Among various methods, the co-precipitation route is very attractive due to its short growth time, low cost and controllable grain size. We have studied how the particle size and defect density vary with calcination temperature and induce changes in structural, optical and magnetic properties. Zn–Cu-codoped SnO_2 nanoparticles are promising for applications in catalysis, optoelectronics and spintronics devices. In the following sections we present our experimental findings along with detailed explanations.

2. Materials and methods

The reagents of $SnCl_2{\cdot}2H_2O$ (98%), $ZnCl_2$ (99%), $CuCl_2$ (99%), and $NH_3{\cdot}H_2O$ (25%–28%) with analytical grade were used as the source materials without further purification. Ultrapure water (18.3 MΩ) was used throughout the experiments. First, 0.22 M of $SnCl_2{\cdot}2H_2O$ was dissolved in 50-ml distilled water, 0.05-M $CuCl_2$ in 25 ml of distilled water

*Project supported by the Natural Science Foundation of Zhejiang Province, China (Grant No. LR16F040001).
†Corresponding author. E-mail: lujianguo@zju.edu.cn
© 2017 Chinese Physical Society and IOP Publishing Ltd

and 0.05-M $ZnCl_2$ in 25 ml of distilled water with continuous stirring. When all are completely dissolved, these solutions were mixed together. Now 35 ml of 2-M NH_4OH solution was added to the above solution by drop wise with continuous stirring and drop rate of 3 ml/minute. Resulting precipitates were collected by centrifugation and washed five to six times with distilled water and dried at 60 °C. Finally the products were calcined at 400 °C and 600 °C to obtain the Zn–Cu-codoped SnO_2 nanoparticles.

The structures of synthesized samples were characterized by an Empyrean 200895 (Netherland) x-ray diffraction (XRD) with Cu $K\alpha$ radiation ($\lambda = 1.5418$ Å). The morphologies of the products were investigated by a Hitachi S-4800 field-emission scanning electron microscope (FE-SEM). High-resolution transmission electron microscopy (HR-TEM) images were recorded from a FEI F20 (USA) system. The chemical composition was analyzed by using an energy dispersive x-ray (EDX) spectroscopy attached to the SEM. The UV-visible diffuse reflectance spectrum (DRS) was obtained from a UV-3600 model spectrophotometer. Fourier transform infrared spectroscopy (FTIR) spectra were obtained by using the FTIR TENSOR 27 system. Raman Spectra were recorded using the LabRamHRUV system. Dc magnetization (M(H)) measurements were carried out using a Quantum Design magnetic properties measurement system (MPMS) at room temperature.

3. Results and Discussion

Figure 1 shows the typical XRD patterns of Zn–Cu-codoped SnO_2 nanoparticles calcined at 400 °C and 600 °C. The peak positions of both samples coincide with the rutile tetragonal structure of SnO_2 (JCPDS No. 41-1445). No impurity peaks are observed corresponding to any metallic cluster or oxide phase, indicating that Zn and Cu have been incorporated in SnO_2 lattice. It can be observed that the intensities of XRD peaks are enhanced while their widths reduced when the calcination temperature is elevated from 400 °C to 600 °C. The average crystallite size, calculated using the Scherer formula, increases from 4.5 nm to 7.3 nm when the calcination temperature is up from 400 °C to 600 °C. The incorporation of Zn and Cu with +2 valence to replace Sn^{4+} in SnO_2 lattice results in the enhancement of densification and oxygen vacancies.[17,18] The ionic radius of Zn^{2+} is 0.074 nm and Cu^{2+} is 0.069 nm, whereas that of Sn^{4+} is 0.069 nm. Therefore Zn^{2+} and Cu^{2+} ions can well substitute the Sn^{4+} in the crystal due to nearly comparable ionic radii.

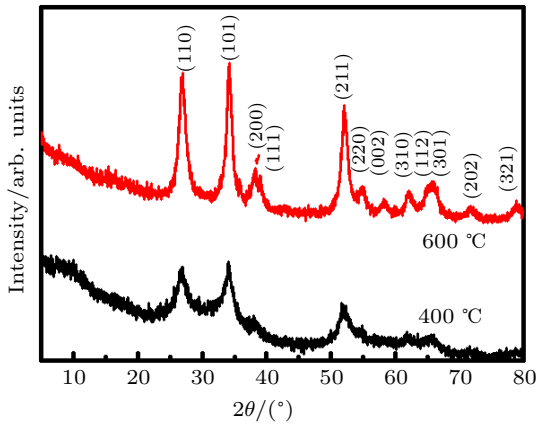


Fig. 1. (color online) XRD spectra of Zn–Cu-codoped SnO_2 nanoparticles calcined at 400 °C and 600 °C.

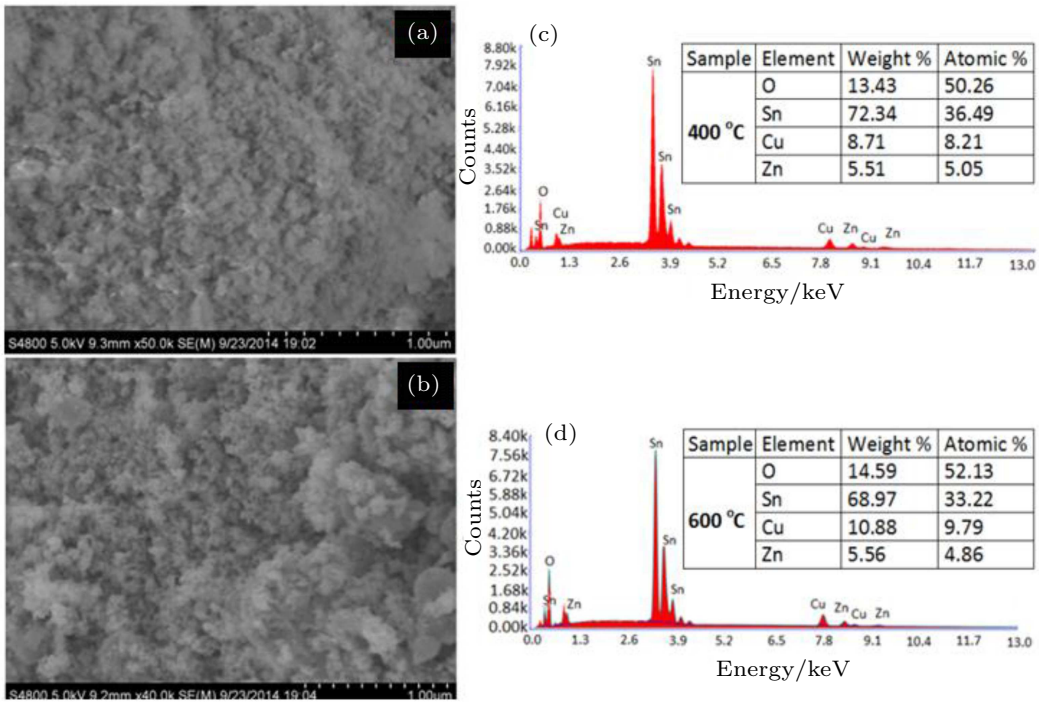


Fig. 2. (color online) FE-SEM images of Zn–Cu-codoped SnO_2 nanoparticles calcined at (a) 400 °C and (b) 600 °C, and EDX patterns of Zn–Cu-codoped SnO_2 nanoparticles calcined at (c) 400 °C and (d) 600 °C with the inset showing the element contents.

Figures 2(a) and 2(b) display the SEM micrographs of Zn–Cu-codoped SnO_2 nanoparticles calcined at 400 °C and 600 °C, respectively. We can see the large aggregates of nanoparticles. The crystallanity increases with increasing calcination temperature. Figures 2(c) and 2(d) exhibit the EDX patterns of two samples, respectively. Signs of elements O, Sn, Zn, and Cu in both samples are observed. The Zn, Cu, and Sn contents are 5.05, 8.21, and 36.49 at.%, respectively in Zn–Cu-codoped SnO_2 nanoparticles calcined at 400 °C, while they are 4.86, 9.79, and 33.22 at.% at 600 °C. The (Zn+Cu+Sn):O atomic ratios are 49.74:50.26 and 47.87:52.13 for Zn–Cu-codoped SnO_2 nanoparticles calcined at 400 °C and 600 °C, respectively, significantly higher than the stoichiometric ratio of 1:2 in intrinsic SnO_2. The fact reveals that the Zn–Cu-codoped SnO_2 nanoparticles are in an oxygen-poor state, having a lot of oxygen vacancies in matrix. Moreover, there are more oxygen vacancies in nanoparticles calcined at 400 °C than those at 600 °C. Thus, the elevation in calcination temperature improves the crystallanity and reduces defects like oxygen vacancies in samples.

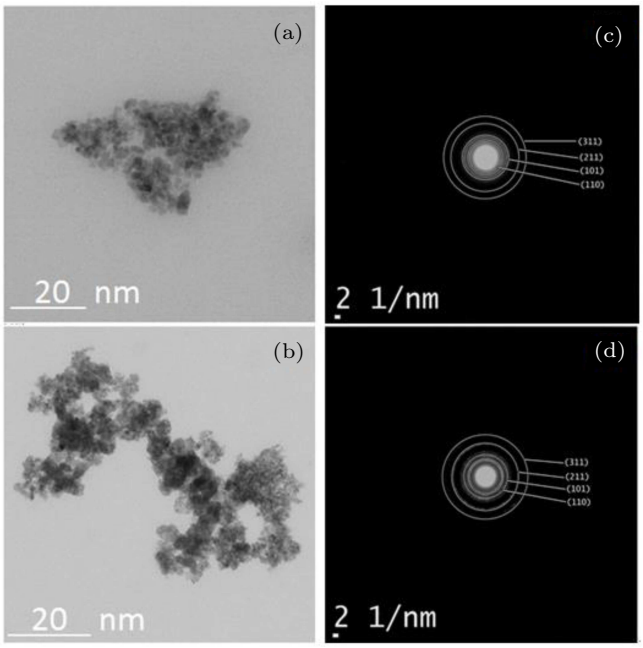


Fig. 3. (color online) TEM images of Zn–Cu-codoped SnO_2 nanoparticles calcined at (a) 400 °C and (b) 600 °C, and SAED patterns of Zn–Cu-codoped SnO_2 nanoparticles calcined at (c) 400 °C and (d) 600 °C.

TEM micrographs of Zn–Cu-codoped SnO_2 nanoparticles are shown in Figs. 3(a) and 3(b). The size enlargement with elevation of calcination temperature indicates the grain growth and improvement in crystallization. The average particle sizes can be estimated by careful identification of nanoparticles in the TEM images, which are determined to be 2.55 nm and 4.13 nm for nanoparticles calcined at 400 °C and 600 °C, respectively. The particle size obtained from TEM is smaller by about a factor of 0.57 as compared with that derived from XRD. This difference is mainly caused by the different particle size criteria, underlying the different methods.[19] In general, the average particle size determined by TEM is smaller than that derived from XRD. Figures 3(c) and 3(d) show the selected area electron diffraction (SAED) patterns of Zn–Cu-codoped SnO_2 nanoparticles calcined at 400 °C and 600 °C, respectively. Fringe patterns corresponding to (110), (101), (211), and (311) planes are consistent with the peaks observed in the XRD patterns. XRD and TEM studies exclude the formation of impurities and firmly confirm the tetragonal structure of SnO_2 nanoparticles for both samples.

In Fig. 4 Raman spectroscopy measurements are performed for Zn–Cu-codoped SnO_2 nanoparticles calcined at 400 °C and 600 °C. The peaks are centered at 474, 630, and 772 cm^{-1} for nanoparticles calcined at 400 °C and 473, 631, and 775 cm^{-1} at 600 °C, which are corresponding to the three fundamental vibrational modes of E_g, A_{1g}, and B_{2g}, respectively. In both samples the peak positions of the three modes correspond to the rutile tetragonal phase of SnO_2 nanocrystal. The same vibrational modes in bulk SnO_2 powder are observed at 474, 638, and 776 cm^{-1}, respectively.[20] In the present case of both samples, the observed peaks are shifted. The shift is associated with the change in grain size. The B_{2g} and E_g modes approach A_{1g}, while A_{1g} shifts to the lower wavenumber with reduction in grain sizes.[21,22] Increasing intensity of A_{1g} mode is the indication of enhancement in crystallanity. Also the intensity of E_g peak (very sensitive to oxygen vacancies) is reduced with increasing calcination temperature, which means oxygen vacancies are reduced in the sample calcined at 600 °C. So the Raman results firmly agree to those of XRD and EDX.

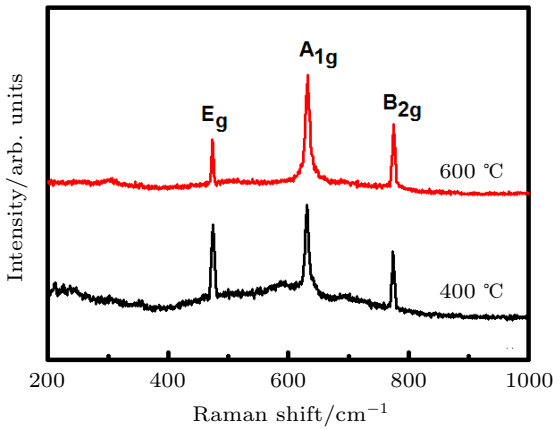


Fig. 4. (color online) Raman spectra of Zn–Cu-codoped SnO_2 nanoparticles calcined at 400 °C and 600 °C.

FTIR is a more sensitive technique as compared to XRD and Raman in characterization of phases and lattice distortions. Figure 5 shows the FTIR spectra recorded in the range 400 cm^{-1}–4000 cm^{-1} in order to confirm the phase purity of Zn–Cu-codoped SnO_2 nanoparticles calcined at 400 °C and 600 °C. The observed broad peak in 530 cm^{-1}–622 cm^{-1} range is due to possible vibrations of Sn–O and O–Sn–O

modes.[23] Peaks at 1032, 1255, 1383, 1448, and 1621 cm^{-1} are due to possible vibrations of Sn–OH and H_2O modes.[23] The broad peak at 3441 cm^{-1} is due to the possible vibrations of Sn–OH mode.[24] The absorption peaks observed between 2300 cm^{-1} and 3000 cm^{-1} are assigned to the CO_2 mode.[25] It is clearly observed from the Fig. 5 that the intensity of IR peaks decreases with increasing calcination temperature. The enhancement in band intensity and band width indicates a reduction in particle size.[26] So the size of the particles calcined at 400 °C is less than the particles calcined at 600 °C. The FTIR analysis strongly supports XRD and TEM analyses.

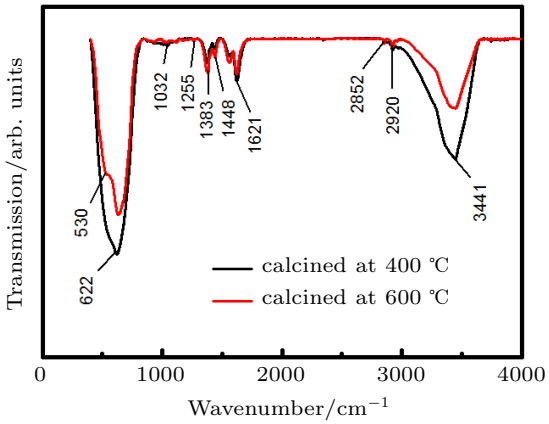


Fig. 5. (color online) FTIR spectra of Zn–Cu-codoped SnO_2 nanoparticles calcined at 400 °C and 600 °C.

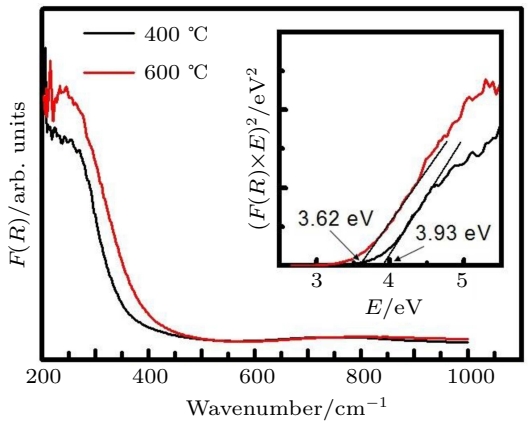


Fig. 6. (color online) Absorption spectra of Zn–Cu-codoped SnO_2 nanoparticles calcined at 400 °C and 600 °C. The inset shows the corresponding plots of $(F(R) \times E)^2$ versus photon energy (E).

The UV–VIS DRS was measured for better understanding of optical properties of Zn–Cu-codoped SnO_2 nanoparticles. Figure 6 shows the absorbance ($F(R)$) of Zn–Cu-codoped SnO_2 nanoparticles calcined at 400 °C and 600 °C. The nanoparticles calcined at 600 °C show larger absorption in the UV light region, which demonstrates the presence of large agglomerates. The absorption edge shifts to longer wavelength in case of sample calcined at 600 °C, with the sharp rise of the absorption edge, revealing the enhancement in crystallanity. It is well known that larger defect density leads to the broadening of the absorption spectra at the absorption edge. Using the Kubelka–Munk equation,[27] the optical band gap energy (E_g) is calculated by plotting $(F(R) \times E)^2$ on vertical-axis and the incident photon energy $E = h\nu$ on horizontal-axis. By extrapolation of the linear portion at $(F(R) \times E)^2 = 0$, the band gap energy can be evaluated, as shown in the inset of Fig. 6. Thus the band gap energy values are found to be 3.93 eV and 3.62 eV for Zn–Cu-codoped SnO_2 nanoparticles calcined at 400 °C and 600 °C, respectively. This means that the band gap energy decreases with increasing calcination temperature. As determined by TEM, the average particle sizes are 2.55 nm and 4.13 nm for nanoparticles calcined at 400 °C and 600 °C, respectively. Thus, the reduction in band-gap is believed to be due to the quantum confinement effect, since as the size of nanoparticles reduces their band gap increases.[28]

Magnetic measurements performed at room temperature for Zn–Cu-codoped SnO_2 nanoparticles are shown in Fig. 7. Both samples exhibit room-temperature ferromagnetism as observed in Fig. 7, which is in accordance to the previous observations of room-temperature magnetism in codoped SnO_2 nanoparticles or thin films as reported by Mehraj *et al.*,[29] Kamble *et al.*,[8] and Chen *et al.*[30] The saturation magnetization (M_s) at room temperature decreases from 0.0037 emu/g to 0.0017 emu/g with increasing calcination temperature from 400 °C to 600 °C. The observed difference between M_s is the clear indication that oxygen vacancies become more active at low calcination temperature of 400 °C, which also induce the ferromagnetism with saturation magnetization of almost 2 times higher magnitude than that at 600 °C. In addition, the observed coercivity field (H_c) decreases from 81.45 emu/g to 76.05 emu/g and the remanent magnetization (M_R) decreases from 5.26 emu/g to 2.4 emu/g as the calcination temperature increases from 400 °C to 600 °C. The enhancement in saturation magnetization, remanent magnetization and coercive field at 400 °C compared with 600 °C is due to the small nanoparticle size and large amount of oxygen vacancies for Zn–Cu-codoped SnO_2 nanoparticles calcined at low temperature.

Based on the XRD, SEM, and TEM data, we can draw the conclusion that Zn–Cu-codoped SnO_2 nanoparticles have been synthesized with spherical shapes. As the calcination temperature increases, the size of nanoparticles is enlarged, leading to the enhanced crystalline quality. The introduction of Zn and Cu into SnO_2 can be well verified by the EDX patterns. Raman and FTIR spectra reveal that the nanoparticles are in an oxygen-poor state having oxygen vacancies at low temperatures. The optical band gap energies are derived from the absorption spectra, which decreases from 3.93 eV to 3.62 eV as the temperatures increase from 400 °C to 600 °C owing to the quantum size effect. The Dc magnetization measurements reveal the nanoparticles have room-temperature ferromagnetism, with a larger saturation magnetization at 400 °C due to the large density of defects such as oxygen vacancies.

All measured data agree well with each other. The optical and ferromagnetic behaviors are in a good agreement with the structural properties.

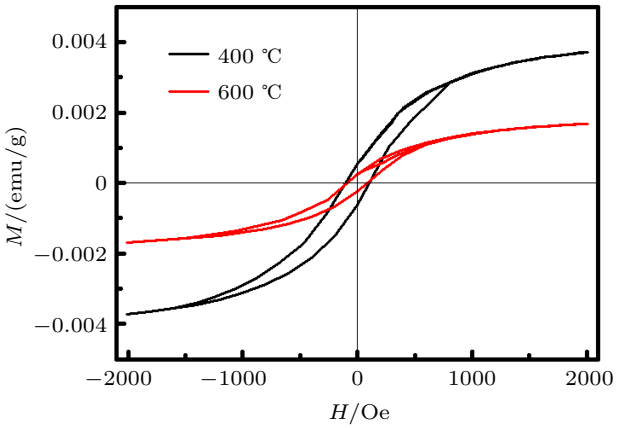


Fig. 7. (color online) Room temperature $M(H)$ loops for Zn–Cu-codoped SnO_2 nanoparticles calcined at 400 °C and 600 °C. The units 1 Oe = 79.5775 A·m^{-1}.

4. Conclusions

In summary, we have synthesized Zn–Cu-codoped SnO_2 nanoparticles at calcination temperatures of 400 °C and 600 °C by the chemical co-precipitation method. The incorporation of Zn and Cu in SnO_2 lattice introduces significant changes in physical properties of the two nanocrystals. The average particle size increases from 2.55 nm to 4.13 nm with reduction in density of oxygen vacancies as calcination temperature increases from 400 °C to 600 °C. The optical band gap energies are 3.93 eV and 3.62 eV for Zn–Cu-codoped SnO_2 nanoparticles calcined at 400 °C and 600 °C, respectively. The increased band gap with reduction in size is due to quantum confinement effects. Both samples show room temperature ferromagnetism, and the sample calcined at 400 °C shows a larger saturation magnetization due to the presence of more defects such as oxygen vacancies. Zn–Cu-codoped SnO_2 nanoparticles with enhanced room-temperature ferromagnetism are the potential candidates having application in the fields of optoelectronics and spintronics.

References

[1] Ansari S A, Khan M M, Ansari M O, Lee J and Cho M H 2014 *New J. Chem.* **38** 2462
[2] Asdim, Manseki K, Sugiura T and Yoshida T 2014 *New J. Chem.* **38** 598
[3] Hays J, Punnoose A, Baldner R, Engelhard M H, Peloquin J and Reddy K M 2005 *Phys. Rev. B* **72** 075203
[4] Ogale S B, Choudhary R J, Buban J P and Lofland S E 2003 *Phys. Rev. Lett.* **91** 077205
[5] Matti A, Mäki J and Rantala T 2001 *Phys. Rev. B* **64** 075407
[6] Chen X, Liu L, Yu P Y and Mao S 2011 *Science* **331** 746
[7] Li L, Liu X, Zhang Y, Nuhfer N T, Barmak K, Salvador P A and Rohrer G S 2013 *ACS Appl. Mater. Interfaces* **5** 5064
[8] Kamble V B and Umarji A M 2013 *AIP Adv.* **3** 082120
[9] Li N, Liu K G, Xie Y, Zhou G, Zhu J, Li F and Cheng H M 2013 *J. Mater. Chem. A* **1** 1536
[10] Ansari S A, Khan M M, Kalathil S, Nisar A, Lee J and Cho M H 2013 *Nanoscale* **5** 9238
[11] Cheng Z D, Tang Z and Zhu J 2011 *Chin. Phys. Lett.* **28** 037501
[12] Xie D N, Peng H S, Huang S H, You F T and Wang X H 2014 *Acta Phys. Sin.* **63** 147801 (in Chinese)
[13] Hu M, Wu Y Q and Tian Y M 2017 *Chin. Phys. B* **26** 020701
[14] Li Q J and Liu B B 2016 *Chin. Phys. B* **25** 076107
[15] Kirszensztejn P, Tolinska A and Przekop R 2009 *Therm. Anal. Calorim.* **95** 93
[16] Jiamiao N, Zhao X and Zhao J 2012 *Surf. Coat. Technol.* **206** 4356
[17] Nomura K, Okabayashi J, Okamura K and Yamada Y 2011 *J. Appl. Phys.* **110** 083901
[18] Cerri J A, Leite E R, Gouvea D and Longo E 1996 *J. Am. Ceram. Soc.* **79** 799
[19] Lu J G, Ye Z Z, Zeng Y J, Zhu L P, Wang L, Yuan J, Zhao B H and Liang Q L 2006 *J. Appl. Phys.* **100** 073714
[20] Mehraj S, Ansari M S and Alimuddin 2015 *Physica E* **65** 84
[21] Sahay P P, Mishra R K, Pandey S N, Jha S and Shamsuddin M 2013 *Current Appl. Phys.* **13** 479
[22] Sinha A K, Manna P K, Pradhan M, Mondal C, Yusuf S M and Pal T 2014 *RSC Adv.* **4** 208
[23] Popescu D A and Verduraz F B 2001 *Catalysis Today* **70** 139
[24] Kittilstved K R, Norberg N S and Gamelin D R 2005 *Phys. Rev. Lett.* **94** 147204
[25] Mehraj S, Ansari M S and Alimuddin 2013 *Physica B* **430** 106
[26] Zulfiqar, Yuan Y L, Jiang Q J, Yang J, Feng L S, Wang W C, Ye Z Z and Lu J G 2016 *J. Mater. Sci.* **27** 9541
[27] Senthilkumar V, Vickraman P and Ravikumar R J 2010 *J. Sol-Gel Sci. Technol.* **53** 316
[28] Kamble V B, Bhatt S V and Umarji A M 2013 *J. Appl. Phys.* **113** 244307
[29] Mehraj S, Anasari M S and Alimuddin 2015 *Thin Solid Films* **589** 57
[30] Yuan C Z, Quan C Z, Kun P R and Jie W S 2013 *Chin. Phys. Lett.* **30** 027804